Received: 14 July 2020 | Accepted: 20 November 2020

DOI: 10.1111/jvim.15984

STANDARD ARTICLE

Journal of Veterinary Internal Medicine Open Access

ACVIM American College of Veterinary Internal Medicine

Utility of tricuspid annular plane systolic excursion normalized by right ventricular size indices in dogs with postcapillary pulmonary hypertension

Yunosuke Yuchi | Ryohei Suzuki | Takahiro Teshima | Hirotaka Matsumoto | Hidekazu Koyama

Faculty of Veterinary Science, Laboratory of Veterinary Internal Medicine, School of Veterinary Medicine, Nippon Veterinary and Life Science University, Tokyo, Japan

Correspondence
Ryohei Suzuki, Faculty of Veterinary Science, Laboratory of Veterinary Internal Medicine, School of Veterinary Medicine, Nippon Veterinary and Life Science University, 1-7-1 Kyonan-cho, Musashino-shi, Tokyo 180-8602, Japan.
Email: ryoheisuzuki@nvlu.ac.jp

Abstract

Background: Tricuspid annular plane systolic excursion (TAPSE) is a common right ventricular (RV) function indicator. However, TAPSE was not decreased in dogs with myxomatous mitral valve disease (MMVD) and postcapillary pulmonary hypertension (PH) because of its load, angle, and body weight dependency, and TAPSE was considered a preload-dependent index.

Objectives: To evaluate the utility of TAPSE normalized by RV size in dogs with postcapillary PH.

Animals: Twenty healthy dogs and 71 MMVD dogs with or without PH.

Methods: In this prospective observational study, end-diastolic RV internal dimension (RVIDd), end-diastolic and end-systolic RV area, and end-diastolic RV wall thickness were measured as RV size indices. The TAPSE was measured using B-mode and M-mode methods. Normalized TAPSE was calculated by dividing TAPSE by each RV size index. The RV strain was obtained as the detailed RV function using 2-dimensional speckle tracking echocardiography. All indices were compared among the PH severity groups and in the presence of right-sided congestive heart failure (R-CHF).

Results: Although nonnormalized TAPSE was higher with PH severity progression, each normalized TAPSE showed a significant decrease in the severe PH group ($P < .05$). The $TAPSE_{B\text{-}mode}$/RVIDd ratio had high area under the curve to predict R-CHF and had moderate correlation with RV strain ($P < .05$). The $TAPSE_{B\text{-}mode}$/RVIDd and left atrial-to-aortic diameter ratios were independent predictors for R-CHF.

Abbreviations: 3seg, only right ventricular free wall analysis; 6seg, global right ventricular analysis; AUC, area under the curve; CI, confidence intervals; CV, coefficient of variation; ICC, intraclass correlation coefficient; IQR, interquartile range; LA/Ao, left atrial-to-aortic diameter ratio; LVIDDN, end-diastolic left ventricular internal diameter normalized by body weight; MMVD, myxomatous mitral valve disease; PH, pulmonary hypertension; R-CHF, right-sided congestive heart failure; ROC, receiver operating characteristic; RV, right ventricular; RVEDA, end-diastolic right ventricular area; RVESA, end-systolic right ventricular area; RVIDd, end-diastolic right ventricular internal dimension; RV-SL, right ventricular longitudinal strain; RVWTd, end-diastolic right ventricular wall thickness; STE, speckle tracking echocardiography; TAPSE, tricuspid annular plane systolic excursion; TAPSE/Ao, tricuspid annular plane systolic excursion-to-aortic diameter ratio; TR, tricuspid regurgitation; TRPG, tricuspid regurgitation pressure gradient; VHS, vertebral heart size.

Conclusions and Clinical Importance: Normalized TAPSE could reflect RV systolic dysfunction in dogs with severe PH, which could not be detected by nonnormalized TAPSE. The $TAPSE_{B\text{-}mode}$/RVIDd ratio might predict R-CHF with high sensitivity and reproducibility.

KEYWORDS

canine, echocardiography, myxomatous mitral valve disease, right ventricular function

1 | INTRODUCTION

Pulmonary hypertension (PH) is a life-threatening complication in dogs with myxomatous mitral valve disease (MMVD) and is characterized by increased pulmonary artery pressure, pulmonary vascular resistance, or both.[1,2] Pulmonary hypertension could induce various changes in the right heart, including right ventricular (RV) hypertrophy, RV dilatation, RV dysfunction, and right-sided congestive heart failure (R-CHF).[1,2] Pulmonary hypertension secondary to left heart disease, commonly known as postcapillary PH, is hemodynamically classified into isolated postcapillary PH and combined postcapillary and precapillary PH.[3-5] Progression to combined postcapillary and precapillary PH, which could be induced by increased pulmonary vascular resistance in addition to increased left atrial pressure, is associated with poor prognosis in affected humans.[6] Although right heart catheterization is the gold standard for the diagnosis of PH,[4,7] it is difficult to implement this procedure in dogs because of the need for anesthesia. Therefore, various echocardiographic indicators have been used to assess PH and its impact on the cardiovascular system in veterinary medicine.[4,5,8-11]

Tricuspid annular plane systolic excursion (TAPSE) is an echocardiographic parameter of RV systolic function.[9,12-15] In human medicine, TAPSE is strongly correlated with RV ejection fraction.[16] In addition, decreased TAPSE is associated with RV systolic dysfunction and heart failure in patients with MMVD and PH.[17,18] However, recent studies have reported that TAPSE was not decreased in dogs with postcapillary PH because of its load, angle, and body weight dependency, and TAPSE was considered a preload-dependent index in dogs.[8,19-21] To eliminate the effect of angle dependency, some reports have assessed the utility of TAPSE measured by B-mode for the assessment of RV systolic function.[13,22] In addition, TAPSE-to-aortic diameter ratio (TAPSE/Ao) enables body weight independent assessment of RV systolic function.[23] Nevertheless, the clinical utility of TAPSE for the assessment of RV function in veterinary medicine is debatable.

Recently, in human medicine, a load-independent assessment of RV function was conducted using echocardiographic indices divided by RV size.[24] We hypothesized that TAPSE normalized by RV size could assess RV systolic function regardless of RV load in dogs as well as in humans. Therefore, we aimed to evaluate the utility of TAPSE normalized by RV size for the assessment of RV systolic function in dogs with MMVD.

2 | MATERIALS AND METHODS

Our study was prospective and observational. Dogs that underwent cardiac screening were recruited at a university veterinary medical hospital in Japan from October 2017 to December 2019. Written informed consent authorizing participation of the dogs in the study was obtained from all of the dogs' owners. All echocardiographic and radiographic indices used in our study were measured by a single observer who was trained by a cardiologist and blinded to the dogs' identities. All echocardiographic examinations were performed by a single investigator, who was different from the investigator who analyzed all of the echocardiographic and radiographic indices.

2.1 | Animals

Client-owned dogs that were clinically healthy or had MMVD were prospectively included in our study. Dogs were diagnosed as clinically healthy based on medical history, physical examination, electrocardiography, radiography, noninvasive blood pressure measurement, and transthoracic echocardiography. Dogs were diagnosed as having MMVD based on the presence of mitral valve thickening or prolapse and mitral regurgitation, as identified using transthoracic echocardiography.[25] If dogs with MMVD also had tricuspid regurgitation (TR), they were deemed as having PH according to TR ≥3.0 m/s (TR pressure gradient [TRPG] ≥36 mmHg). Dogs that had other cardiac diseases, diseases that might affect the cardiac function or pulmonary artery pressure (eg, respiratory disease, thromboembolic disease, heartworm disease, neoplastic disease, endocrine disease), and systemic hypertension (systolic blood pressure ≥160 mmHg)[26] were excluded from the study along with cases that had missing data.

Dogs with MMVD were divided into 3 groups based on the American College of Veterinary Internal Medicine consensus: stage B1 consisted of asymptomatic dogs with no or minimal remodeling, stage B2 consisted of asymptomatic dogs with substantial remodeling based on radiography and echocardiography, and stage C/D consisted of symptomatic dogs with current or past clinical signs of heart failure caused by MMVD.[27] In addition, dogs with MMVD were classified into 4 groups based on TRPG: non-PH, defined as TRPG <36 mmHg or absence of TR; mild PH, defined as TRPG of 36 to 50 mmHg; moderate PH, defined as TRPG of 50 to 75 mmHg; and severe PH, defined as TRPG >75 mmHg.[5,12] Furthermore, dogs with TR were classified

qualitatively according to TR severity using color Doppler and continuous wave Doppler methods: mild TR consisted of dogs with a small TR jet based on color Doppler and a faint parabolic TR jet signal based on the continuous wave Doppler; moderate TR consisted of those with an intermediate TR jet and a dense parabolic TR jet signal; and severe TR consisted of those with a substantial large central or eccentric wall-impinging TR jet and a dense triangular, early-peaking TR jet signal.[28,29] Dogs were diagnosed as having left-sided congestive heart failure if they had at least 1 clinical sign, such as tachypnea, respiratory distress, or exercise intolerance, supported by radiographic and ultrasonographic evidence of pulmonary venous congestion and pulmonary edema. Dogs were diagnosed as having R-CHF if they had at least 1 radiographic and ultrasonographic finding indicative of ascites, pleural effusion or pericardial effusion or clinical signs of cardiac syncope, jugular venous congestion, or peripheral edema without any evidence of diseases except for PH, other than neurological diseases.

2.2 | Clinical and radiographic examinations

All dogs underwent complete physical examination and blood pressure measurement using the oscillometric method on the same day as echocardiographic evaluation. Dogs underwent blood examinations, neurological examinations or both for differential diagnosis of diseases listed in the exclusion criteria whenever necessary. If dogs had any echocardiographic evidence of thrombosis, such as intracardiac thrombus and smoke-like echo, we also performed blood clotting tests. To eliminate the possibility of thromboembolic disease, dogs that had abnormally high concentrations of fibrin degradation products (>4.0 μg/mL) and D-dimers (>2.0 μg/mL) were excluded from the study. Thoracic radiography was performed to measure vertebral heart size (VHS).[30] Abdominal radiography was performed to assess the presence of ascites when necessary. Abdominal ultrasonography was performed to assess the presence of ascites and congestion of the caudal vena cava and hepatic vein using the caudal vena cava subxiphoid point-of-care ultrasound view, as reported previously.[31,32]

2.3 | Standard echocardiography

Conventional 2-dimensional (2D), M-mode, and Doppler examinations were performed using a Vivid E95 echocardiographic system (GE Healthcare, Tokyo, Japan) and a 3.5- to 6.9-MHz transducer. Lead II ECG was recorded simultaneously and displayed on the images. All of the data were stored and obtained from at least 5 consecutive cardiac cycles in sinus rhythm from nonsedated dogs that were manually restrained in right and left lateral recumbency. Images were analyzed using an offline workstation (EchoPAC PC, Version 203; GE Healthcare).

For the described echocardiographic indices, mean values obtained from 3 consecutive cardiac cycles from high-quality images were used. The left atrial-to-aortic diameter ratio (LA/Ao) was obtained from the right parasternal short-axis view using the B-mode method.[33-35] The end-diastolic left ventricular internal diameter normalized by body weight (LVIDDN) was obtained from the right parasternal short-axis view at the level of the chordae tendineae using B-mode and the inner edge-to-inner edge method; LVIDDN = (end-diastolic left ventricular internal dimension)/(body weight [kg])$^{.294}$.[36] Peak TR velocity was obtained from the right parasternal long-axis view, short-axis view at the level of the heart base, or left parasternal apical 4-chamber view optimized for the right heart (RV focus view). The RV focus view was obtained by adapting the left parasternal apical 4-chamber view for the right heart, as described previously.[12,37,38] Systolic pulmonary artery pressure was estimated by calculating peak TRPG using the simplified Bernoulli equation: TRPG (mmHg) = 4 × (TR peak velocity [m/s])$^{.239}$

2.4 | Measurement of RV morphological and functional indicators

All of the echocardiographic indices were obtained using the same ultrasound and offline workstation as the standard echocardiography. To eliminate the effect of respiratory variation, the mean of 5 consecutive cardiac cycles in sinus rhythm from the high-quality images were used for statistical analyses.

For indicators of RV size, the following indices were measured using RV focus view: RV end-diastolic internal dimension (RVIDd), RV end-diastolic and end-systolic area (RVEDA and RVESA, respectively), and RV wall thickness (RVWTd; Figure 1A).[12,37,38] The RVIDd was measured as the largest diameter at the middle RV parallel to the tricuspid annulus using the B-mode method. The RVEDA and RVESA were measured by tracing the endocardial border of the RV inflow region, excluding the papillary muscles, at end-diastole and end-systole, respectively.[12,28] The RVWTd was the RV free wall thickness at end-diastole measured at the level of the largest RV diameter using the B-mode method.

The TAPSE was measured using B-mode and M-mode methods ($TAPSE_{B\text{-}mode}$ and $TAPSE_{M\text{-}mode}$, respectively) using the RV focus view (Figure 1B) and was measured during the same cardiac cycles as the RV size measurements. The TAPSE was defined as the total displacement of the lateral tricuspid annulus. The $TAPSE_{B\text{-}mode}$ was measured by tracing the distance of the lateral tricuspid annulus when cine-loops advanced from end-diastole to end-systole.[13,22] The M-mode images were constructed using B-mode cine-loops that were used for $TAPSE_{B\text{-}mode}$ by setting the cursors at the RV apex and lateral tricuspid annulus.[13] The TAPSE/Ao ratio was calculated by dividing TAPSE by aortic diameter obtained from the right parasternal short-axis view.[23] In addition, TAPSE normalized using RV size was calculated by dividing TAPSE by each RV size index in the same cardiac cycle.

2.5 | 2D speckle tracking echocardiography

All 2D speckle tracking echocardiography (2D-STE) analyses were performed by the same investigator using the same ultrasound

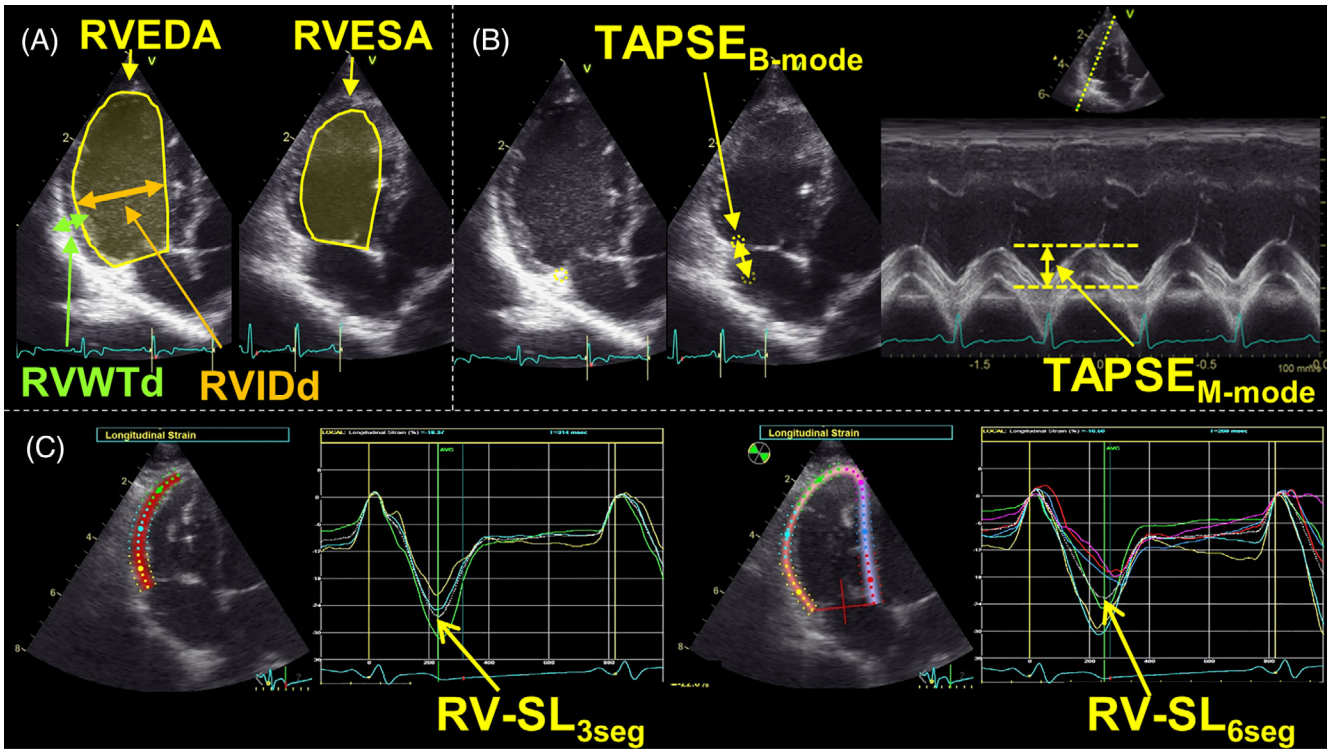

FIGURE 1 Echocardiographic indices for RV morphology and function measured in this study: RV size indicators (RVIDd, RVEDA, RVESA, RVWTd), A, TAPSE measured using B-mode and M-mode methods, B, and RV-SL obtained by 2-dimensional speckle tracking echocardiography, C. RV, right ventricular; RVEDA, right ventricular end-diastolic area; RVESA, right ventricular end-systolic area; RVIDd, end-diastolic right ventricular diameter; RV-SL; right ventricular peak strain; RVWTd, right ventricular end-diastolic wall thickness; TAPSE, tricuspid annular plane systolic excursion

machine and offline workstation as for standard echocardiography. The RV longitudinal strain value was obtained from the RV focus view using left ventricular 4-chamber algorithms.[25] The region of interest for 2D-STE was defined by manually tracing the RV endocardial border. The RV free wall (3-segment) longitudinal strain (RV-SL_{3seg}) analysis was performed by tracing from the level of the lateral tricuspid annulus to the RV apex. In addition, RV global (6-segment) longitudinal strain (RV-SL_{6seg}) analysis was performed by tracing from the lateral tricuspid annulus to the septal tricuspid annulus (including the interventricular septum) via the 6 segments of the RV apex. Manual adjustments were made for including and tracking the entire myocardial thickness over the cardiac cycle when necessary. When the automated software could not track the myocardial regions, the regions of interest were retraced and recalculated. The RV-SL was defined as the absolute value of the negative peak obtained from the strain wave (Figure 1C).

2.6 | Intraobserver and interobserver measurement variability

Intraobserver measurement of variability was performed by a single observer who performed all of the echocardiographic and radiographic measurements. The RV morphological and functional indices were obtained from the 10 dogs, whereby each of the 2 dogs was randomly selected from the normal and PH severity group and was measured on 2 different days at >7-day intervals, using the same echocardiogram and heart cycles. A second blinded observer measured the same indices for determination of interobserver variability using the same echocardiogram and heart cycles. The reproducibility of $TAPSE_{M\text{-}mode}$ was assessed by constructing an M-mode view using B-mode cine-loops.

2.7 | Statistical analysis

All statistical analyses were performed using commercially available software (EZR software version 1.41).[40] Categorical data were reported as absolute numbers and frequencies as percentages. Continuous data were reported as the median (interquartile range [IQR]).

The normality of data was tested using the Shapiro-Wilk test. Chi-squared or Fisher's exact tests were used for comparing categorical indices among the PH severity groups. Continuous indices were compared between the normal and each PH severity group using 1-way analysis of variance with subsequent pairwise comparisons using Tukey's multiple comparison test for normally distributed data or the Kruskal-Wallis test with subsequent pairwise comparisons using the Steel-Dwass test for nonnormally distributed data. To

predict R-CHF onset, all RV morphological and functional indices were compared for the presence or absence of R-CHF using a Student *t* test for normally distributed data or the Mann-Whitney *U* test for nonnormally distributed data. In addition, multivariate logistic regression analysis using a backward stepwise approach was performed to identify independent predictors of R-CHF onset. Indices that showed significance in the univariate analysis were entered into the multivariate analysis, and those that had coefficients of correlation $|r| > .7$ were not enrolled owing to multicollinearity. Indices entered into the logistic regression analysis were recorded as adjusted odds ratios and their respective 95% confidence intervals (CI). Furthermore, receiver operating characteristic (ROC) curves were created for calculating the area under the curve (AUC), sensitivity, and specificity, and for determining the optimal cutoff values required for estimation of the R-CHF onset. The AUC was considered to have high accuracy if it was > 0.9, moderate accuracy for 0.7 to 0.9, and low accuracy for 0.5 to 0.7.[41] The optimal cutoff value was defined as that which minimized the distance between the curve and the upper left corner in the ROC curve. Linear regression analysis was performed to evaluate correlations between RV-SL and TAPSE, which had the highest AUC for predicting R-CHF onset. Correlation was considered to be strong if the absolute value of correlation coefficient $|r|$ was > 0.7, moderate for 0.4 to 0.7, weak for 0.2 to .4, and no correlation for < 0.2.

Intraobserver and interobserver measurement variability was quantified by the coefficient of variation (CV) and was calculated using the following formula: CV = (SD)/(mean value) × 100. Reproducibility also was evaluated using intraclass correlation coefficients case 1 (ICC [1]) for intraobserver measurement of variability and ICC case 2 (ICC [1, 2]) for interobserver measurement of variability. Good reproducibility was defined as a CV <10.0 and ICC >0.7. Statistical significance was set at $P < .05$.

3 | RESULTS

3.1 | Clinical profiles and standard echocardiography

Twenty healthy dogs and 96 dogs with MMVD met the inclusion criteria. However, 25 dogs with MMVD were excluded based on the exclusion criteria: respiratory disease (n = 11), respiratory disease and endocrine disease (n = 3), endocrine disease (n = 3), endocrine disease and abnormally high concentrations of fibrin degradation products and D-dimers (n = 2), systemic hypertension (n = 1), and missing data (n = 5). Finally, 20 healthy dogs and 71 dogs with MMVD (non-PH, n = 27; mild PH, n = 22; moderate PH, n = 11; and severe PH, n = 11) were enrolled in the study. Dogs consisted of the following breeds: Chihuahua (n = 26, 29%), mixed breed (n = 11, 12%), Toy Poodle (n = 8, 9%), Shih Tzu (n = 6, 7%), Miniature Dachshund (n = 6, 7%), Maltese (n = 5, 5%), Papillon (n = 4, 4%), Miniature schnauzer (n = 4, 4%), Pomeranian (n = 3, 3%), Cavalier King Charles spaniel (n = 2, 2%), Chinese Crested dog (n = 2, 2%), Norfolk terrier (n = 2, 2%), Pekingese (n = 2, 2%), Miniature Pinscher (n = 2, 2%), and 1 dog each from 8 other breeds. Clinical and selected echocardiographic indices for the

TABLE 1 Clinical and selected echocardiographic variables obtained from normal dogs and dogs with various PH severities

	Group					
Variable	Normal	Non-PH	Mild PH	Moderate PH	Severe PH	*P**
n	20	27	22	11	11	
Age (year)	11.6 (9.7-13.1)	11.4 (10.3-14.0)	11.7 (10.6-12.7)	12.9 (12.1-13.2)	14.0 (13.3-14.7)	.05
Sex (male/female)	8/12	15/12	10/11	7/4	7/4	.58
Body weight (kg)	5.6 (3.9-6.7)	4.6 (3.5-5.9)	4.4 (3.5-5.9)	5.9 (3.3-7.3)	3.7 (2.4-7.0)	.39
Heart rate (bpm)	129 (100-143)	114 (92-128)	136 (114-150)	120 (97-143)	129 (118-143)	.21
ACVIM (B1/B2/C/D)	0/0/0	12/11/4	8/10/4	1/3/7	0/1/10	<.01
TR (mild/moderate/severe)	0/0/0	14/4/0	16/6/0	5/6/0	0/4/7	<.01
TR velocity (m/s)		2.6 (2.4-2.8)	3.2 (3.1-3.3)[a]	3.7 (3.6-3.8)[a,b]	5.0 (4.7-5.1)[a,b,c]	<.01
R-CHF (present/absent)	0/20	0/27	0/22	1/10	10/1	<.01
VHS (v)	10.0 (9.7-10.5)	10.6 (10.1-11.1)	10.9 (10.4-11.2)[d]	11.8 (11.2-12.7)[a,b,d]	11.9 (11.6-12.4)[a,b,d]	<.01
LA/Ao	1.3 (1.1-1.3)	1.6 (1.2-1.9)	1.7 (1.3-2.2)[b]	2.2 (1.9-2.3)[d]	1.8 (1.7-2.3)[d]	<.01
LVIDDN	1.4 (1.3-1.4)	1.7 (1.5-2.0)[d]	1.8 (1.4-2.2)[d]	2.0 (1.6-2.3)[d]	1.8 (1.3–2.2)	<.01

Note: Continuous variables are displayed as median (IQR).
Abbreviations: IQR, interquartile range; LA/Ao, left atrium to aortic ratio; LVIDDN, left ventricular end diastolic size normalized by body weight; PH, pulmonary hypertension; R-CHF, right-sided congestive heart failure; TR, tricuspid regurgitation; VHS, vertebral heart size.
[a]The value is significantly different from non-PH ($P < .05$).
[b]The value is significantly different from mild PH ($P < .05$).
[c]The value is significantly different from moderate PH ($P < .05$).
[d]The value is significantly different from Normal ($P < .05$).
*P value of 1-way analysis of variance or Kruskal-Wallis test for continuous data and chi-squared or Fisher's exact tests for categorical data.

left heart are summarized in Table 1. No significant differences in age, sex, body weight, and heart rate were found among the normal and PH severity groups. The population with severe MMVD (C/D group) and TR was significantly higher in the severe PH group (both $P < .01$). Seventy-three percent of the dogs with MMVD were receiving some medical treatments from the referral hospitals at the time of examination: angiotensin-converting enzyme inhibitors (n = 52), pimobendan (n = 32), pulmonary vasodilator (sildenafil; n = 10), loop diuretics (n = 6), or some combination of these. The TR velocity was significantly different among each of the PH severity groups (all $P < .01$). Ten of the 11 dogs with severe PH had at least 1 indicator of R-CHF at the time of the visit: syncope (n = 8), ascites (n = 5), pleural effusion (n = 2), pericardial effusion (n = 2), or some combination of these. The VHS was significantly higher in the mild PH group compared with that of the normal group ($P < .01$) and was higher in the moderate and severe PH groups compared with that of the normal, non-PH, and mild PH groups (all $P < .01$). The LA/Ao was significantly higher in the mild, moderate, and severe PH groups compared with that of the normal group (all $P < .01$). The LVIDDN was significantly lower in the normal group compared with that of the non-PH, mild PH, and moderate PH groups (all $P < .01$).

3.2 | RV morphological and functional indices

The results of RV morphological and functional indices classified by MMVD severity are summarized in Table 2. For the RV morphological indices, RVIDd was significantly higher in the C/D group compared with that of the B1 and B2 groups (both $P < .01$). The RVWTd also was significantly higher in the C/D group compared with that of the other groups (all $P < .01$). The TAPSE measured using B-mode and M-mode methods was significantly higher in the C/D group compared with that of the normal and B1 groups ($TAPSE_{B\text{-}mode}$, $P = .02$ and $P = .04$; $TAPSE_{M\text{-}mode}$, $P < .01$ and $P = .04$). The TAPSE/Ao ratio also increased as MMVD progressed. Conversely, all of the TAPSE values normalized by each RV size had no indication of significant increase in the C/D group, but almost all of these indices were significantly higher in the B2 group compared with those of the

TABLE 2 Results of RV morphological and functional indices in dogs with various MMVD severities

	Group				
Variable	Normal	B1	B2	C/D	P*
RVIDd (mm)	10.1 (9.6-11.8)	10.0 (8.5-11.1)	9.4 (8.1-11.2)	14.1 (10.0-17.6)[a,b]	<.01
RVEDA (cm^2)	2.2 (1.6-2.9)	2.0 (1.6-2.8)	2.1 (1.6-2.7)	2.9 (1.7-4.1)	.09
RVESA (cm^2)	1.0 (0.8-1.5)	1.0 (0.8-1.5)	1.0 (0.7-1.5)	1.3 (0.8-2.3)	.19
RVWTd (mm)	3.5 (3.2-3.8)	3.3 (2.9-3.4)	3.5 (3.2-3.9)	4.1 (3.9-5.2)[a,b,c]	<.01
$TAPSE_{B\text{-}mode}$ (mm)	10.0 (7.8-12.6)	10.3 (8.6-11.3)	12.1 (10.3-13.2)	11.9 (9.2-14.4)[a,c]	<.01
$TAPSE_{B\text{-}mode}$/Ao	0.72 (0.54-0.93)	0.74 (0.65-0.82)	0.91 (0.82-0.98)[a]	0.90 (0.67-1.14)	<.01
$TAPSE_{B\text{-}mode}$/RVIDd	0.94 (0.73-1.11)	0.95 (0.87-1.20)	1.18 (1.06-1.43)[c]	0.88 (0.65-1.27)[b]	<.01
$TAPSE_{B\text{-}mode}$/RVEDA	4.4 (3.0-5.6)	4.9 (4.1-5.8)	5.3 (4.4-7.2)	3.9 (2.5-6.5)	.06
$TAPSE_{B\text{-}mode}$/RVESA	9.4 (5.2-13.3)	9.4 (7.3-10.9)	11.0 (8.2-14.9)	9.3 (4.4-14.5)	.26
$TAPSE_{B\text{-}mode}$/RVWTd	2.8 (2.1-3.3)	3.2 (2.7-3.4)	3.4 (3.0-3.8)	2.6 (2.2-3.4)	.03
$TAPSE_{M\text{-}mode}$ (mm)	8.4 (7.4-10.1)	9.3 (7.8-10.6)	10.4 (8.9-12.0)[c]	10.9 (9.5-13.5)[a,c]	<.01
$TAPSE_{M\text{-}mode}$/Ao	0.64 (0.53-0.82)	0.69 (0.59-0.76)	0.81 (0.68-0.89)[a,c]	0.92 (0.62-1.05)[a,c]	<.01
$TAPSE_{M\text{-}mode}$/RVIDd	0.86 (0.67-1.01)	0.91 (0.77-1.04)	1.10 (0.91-1.30)[c]	0.78 (0.60-1.19)	.01
$TAPSE_{M\text{-}mode}$/RVEDA	3.9 (2.8-5.1)	4.4 (4.0-5.2)	4.5 (4.0-6.6)	3.8 (3.0-6.1)	.12
$TAPSE_{M\text{-}mode}$/RVESA	7.6 (5.5-12.2)	8.0 (7.1-10.1)	9.1 (7.8-15.4)	9.3 (4.7-14.4)	.31
$TAPSE_{M\text{-}mode}$/RVWTd	2.4 (2.1-2.8)	2.8 (2.4-3.2)	3.1 (2.6-3.4)[c]	2.4 (2.0-3.3)	.03
$RV\text{-}SL_{3seg}$ (%)	26.4 (21.4-32.2)	27.3 (23.9-31.5)	30.7 (26.3-35.1)	30.1 (23.51-35.1)	.57
$RV\text{-}SL_{6seg}$ (%)	24.7 (18.0-27.2)	25.6 (19.8-28.3)	26.6 (23.7-31.4)	23.7 (15.3-27.4)	.08

Note: Continuous variables are displayed as median (IQR).

Abbreviations: 3seg, only right ventricular free wall; 6seg, right ventricular free wall and interventricular septum; IQR, interquartile range; MMVD, myxomatous mitral valve disease; RV, right ventricular; RVEDA, right ventricular end-diastolic area; RVESA, right ventricular end-systolic area; RVIDd, end-diastolic right ventricular diameter; RV-SL; right ventricular peak strain; RVWTd, right ventricular end-diastolic wall thickness; TAPSE, tricuspid annular plane systolic excursion.

[a]The value is significantly different from B1 ($P < .05$).

[b]The value is significantly different from B2 ($P < .05$).

[c]The value is significantly different from normal ($P < .05$).

*P value of 1-way analysis of variance or Kruskal-Wallis test.

TABLE 3 Results of RV morphological and functional indices in dogs with various PH severities

Variable	Group					
	Normal	Non-PH	Mild PH	Moderate PH	Severe PH	*P**
RVIDd (mm)	10.0 (9.6-11.8)	9.3 (8.3-11.0)	10.0 (8.7-11.2)	12.3 (9.6-14.5)	16.5 (13.0-20.9)[b,c,d]	<.01
RVEDA (cm^2)	2.2 (1.6-2.9)	1.9 (1.6-2.5)	2.4 (1.6-2.9)	2.9 (1.5-3.8)	3.2 (2.6-5.1)	.05
RVESA (cm^2)	1.0 (0.8-1.5)	1.0 (0.8-1.3)	1.1 (0.7-1.5)	1.2 (0.8-2.0)	1.9 (1.3-3.4)	.05
RVWTd (mm)	3.5 (3.2-3.8)	3.4 (3.1-3.7)	3.5 (3.3-4.0)	4.0 (3.6-4.9)	4.8 (4.1-5.2)[b,c,d]	<.01
RV-SL_{3seg} (%)	26.4 (21.4-32.2)	28.4 (23.0-33.7)	30.9 (25.5-32.3)	34.6 (30.1-38.9)	25.5 (23.8-26.3)[c]	.04
RV-SL_{6seg} (%)	24.7 (18.0-27.2)	26.2 (20.9-28.4)	26.4 (24.1-31.3)	28.2 (23.9-32.2)	16.3 (14.0-22.5)[a,b,c,d]	<.01

Note: Continuous variables are displayed as median (IQR).
Abbreviations: 3seg, only right ventricular free wall; 6seg, right ventricular free wall and interventricular septum; IQR, interquartile range; PH, pulmonary hypertension; RV, right ventricular; RVEDA, right ventricular end-diastolic area; RVESA, right ventricular end-systolic area; RVIDd, end-diastolic right ventricular diameter; RV-SL; right ventricular peak strain; RVWTd, right ventricular end-diastolic wall thickness.
[a]The value is significantly different from non-PH ($P < .05$).
[b]The value is significantly different from mild PH ($P < .05$).
[c]The value is significantly different from moderate PH ($P < .05$).
[d]The value is significantly different from normal ($P < .05$).
*P value of 1-way analysis of variance or Kruskal-Wallis test.

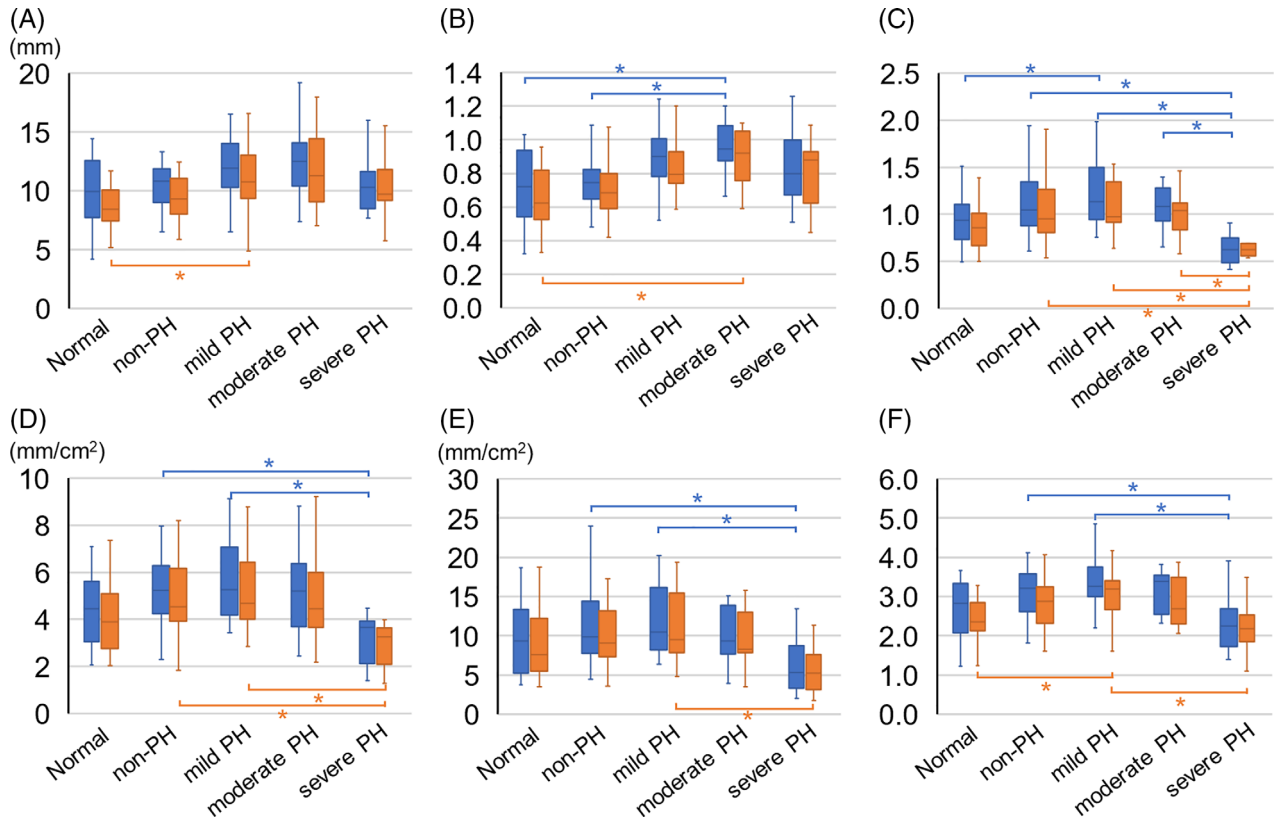

FIGURE 2 Box and whisker plots of the nonnormalized TAPSE and TAPSE normalized by each RV size indicators: TAPSE, A, TAPSE/Ao, B, TAPSE/RVIDd, C, TAPSE/RVEDA, D, TAPSE/RVESA, E, and TAPSE/RVWTd, F. The bottom of the box is the 25%, the middle line is the median, the top of the box is the 75%, and the whiskers represent range. Blue box plots represent $TAPSE_{B\text{-mode}}$, and orange box plots represent $TAPSE_{M\text{-mode}}$. Asterisk symbol (*) indicates that the values differed significantly ($P < .05$) between PH severity groups. The sign in blue and orange indicate significant differences in $TAPSE_{B\text{-mode}}$ and $TAPSE_{M\text{-mode}}$ indices, respectively. PH, pulmonary hypertension; RV, right ventricular; RVEDA, right ventricular end-diastolic area; RVESA, right ventricular end-systolic area; RVIDd, end-diastolic right ventricular diameter; RVWTd, right ventricular end-diastolic wall thickness; TAPSE, tricuspid annular plane systolic excursion; TAPSE/Ao, tricuspid annular plane systolic excursion-to-aortic diameter ratio

normal group. The RV-SL showed no significant differences among the MMVD severity groups.

All of the RV morphological and functional indices classified by PH severity are summarized in Table 3 and Figure 2. For the RV morphological indices, RVIDd and RVWTd were significantly higher as PH severity progressed. The TAPSE measured using M-mode was significantly higher in the mild PH group compared with the normal group (P = .02). The TAPSE/Ao ratio measured using B-mode and M-mode was also significantly higher in the moderate PH group compared with the normal group (both P < .01). However, these indices showed no indication of significant decrease in the severe PH group. In contrast, normalized TAPSE, especially $TAPSE_{B\text{-}mode}$/RVIDd, was higher in the mild PH group compared with that of the normal group (P = .03) and was significantly lower in the severe PH group compared with the non-PH, mild PH, and moderate PH groups (vs non-PH, P < .01; vs mild PH, P < .01; vs moderate PH, P = .01). For RV-SL, although both $RV\text{-}SL_{3seg}$ and $RV\text{-}SL_{6seg}$ tended to be higher in the mild-to-moderate PH and lower in the severe PH, $RV\text{-}SL_{6seg}$ decreased more significantly in the severe PH group.

Regarding results comparing echocardiographic indices according to the existence of R-CHF, all of the RV morphological indices were significantly higher in dogs with R-CHF (RVIDd, 16.5 [14.3-21.3] vs 10.0 [8.6-11.5], P < .01; RVEDA, 3.2 [2.6-5.5] vs 2.1 [1.6-3.0], P = .02; RVESA, 1.8 [1.3-3.7] vs 1.0 [0.8-1.5], P = .02; RVWTd, 4.8 [4.1-5.3] vs 3.5 [3.2-3.9], P < .01). The TAPSE and TAPSE/Ao ratio measured using the B-mode and M-mode methods showed no significant differences between dogs with and without R-CHF ($TAPSE_{B\text{-}mode}$, 11.2 [8.9-12.1] vs 10.8 [9.0-13.0], P = .74; $TAPSE_{M\text{-}mode}$, 9.9 [9.6-12.3] vs 9.6 [7.9-11.6], P = .33; $TAPSE_{B\text{-}mode}$/Ao, 0.80 [0.67-1.00] vs 0.82 [0.69-0.97], P = .94; $TAPSE_{M\text{-}mode}$/Ao, 0.88 [0.62-0.96] vs 0.74 [0.59-0.87], P = .16). In contrast, all of the normalized TAPSE showed significant decreases in dogs with R-CHF ($TAPSE_{B\text{-}mode}$/RVIDd, 0.65 [0.55-0.75] vs 1.05 [0.88-1.32], P < .01; $TAPSE_{B\text{-}mode}$/RVEDA, 3.7 [2.4-3.9] vs 5.2 [4.0-6.6], P < .01; $TAPSE_{B\text{-}mode}$/RVESA, 5.3 [3.6-9.6] vs 10.3 [7.3-14.5], P < .01; $TAPSE_{B\text{-}mode}$/RVWTd, 2.3 [2.0-2.7] vs 3.2 [2.6-3.6], P < .01; $TAPSE_{M\text{-}mode}$/RVIDd, 0.62 [0.58-0.69] vs 0.93 [0.80-1.22], P < .01; $TAPSE_{M\text{-}mode}$/RVEDA, 3.2 [2.4-3.6] vs 4.4 [3.8-6.1], P = .01; $TAPSE_{M\text{-}mode}$/RVESA, 5.2 [3.5-9.4] vs 8.5 [6.7-13.5], P = .03; $TAPSE_{M\text{-}mode}$/RVWTd, 2.2 [1.9-2.5] vs 2.8 [2.3-3.2], P = .05). For RV-SL, only $RV\text{-}SL_{6seg}$ showed a significant decrease in dogs with R-CHF (17.3 [13.0-24.9] vs 25.4 [20.2-30.1], P < .01), although $RV\text{-}SL_{3seg}$ showed no significant decrease (26.0 [24.1-30.6] vs 28.8 [23.2-34.0], P = .27). Table 4 shows the results of univariate and multivariate analyses to identify an independent predictor of R-CHF onset. After excluding the effect of multicollinearity, age, LA/Ao, RVIDd, $TAPSE_{B\text{-}mode}$/RVIDd, $TAPSE_{B\text{-}mode}$/RVWTd, and $RV\text{-}SL_{6seg}$ were enrolled into the multivariate analysis. The $TAPSE_{B\text{-}mode}$/RVIDd and LA/Ao ratios were the significant independent predictors. Results of the ROC curve and optimal cut-off values to predict R-CHF onset are summarized in Table 5 and Figure 3. Normalized TAPSE,

TABLE 4 Results of multivariate analysis to identify the independent predictor of the R-CHF onset

	Univariate analysis		Multivariate analysis	
Variable	**odds ratio (95% CI)**	***P***	**odds ratio (95% CI)**	***P***
Age (year)	1.6 (1.1-2.3)	.01		
LA/Ao (.1)	1.1 (1.0-1.3)	.02	1.6 (1.2-2.1)	<.01
RVIDd (mm)	1.6 (1.2-2.0)	<.01		
RVEDA (cm^2)	2.0 (1.3-3.1)	<.01		
RVESA (cm^2)	3.1 (1.5-6.3)	<.01		
RVWTd (0.1 mm)	1.2 (1.1-1.3)	<.01		
$TAPSE_{B\text{-}mode}$/RVIDd (0.1)	2.1 (1.4-3.1)	<.01	3.7 (1.6-8.2)	<.01
$TAPSE_{B\text{-}mode}$/RVEDA (mm/cm^2)	2.2 (1.3-3.6)	<.01		
$TAPSE_{B\text{-}mode}$/RVESA (mm/cm^2)	1.3 (1.1-1.7)	<.01		
$TAPSE_{B\text{-}mode}$/RVWTd	4.3 (1.6-11.6)	<.01		
$TAPSE_{M\text{-}mode}$/RVIDd (0.1)	1.8 (1.2-2.6)	<.01		
$TAPSE_{M\text{-}mode}$/RVEDA (mm/cm^2)	1.8 (1.1-2.8)	.02		
$TAPSE_{M\text{-}mode}$/RVESA (mm/cm^2)	1.3 (1.0-1.5)	.03		
$TAPSE_{M\text{-}mode}$/RVWTd	2.9 (1.0-8.0)	.04		
$RV\text{-}SL_{6seg}$ (%)	1.2 (1.1–1.3)	<.01		
TR velocity (0.1 m/s)	1.4 (1.2-1.6)	<.01		

Abbreviations: 6seg, right ventricular free wall and interventricular septum; CI, confidence interval; IQR, interquartile range; LA/Ao, left atrium to aortic ratio; PH, pulmonary hypertension; R-CHF, right-sided congestive heart failure; RV, right ventricular; RVEDA, right ventricular end-diastolic area; RVESA, right ventricular end-systolic area; RVIDd, end-diastolic right ventricular diameter; RV-SL; right ventricular peak strain; RVWTd, right ventricular end-diastolic wall thickness; TAPSE, tricuspid annular plane systolic excursion; TR, tricuspid regurgitation; VHS, vertebral heart size.

TABLE 5 Results of receiver operating characteristic curves of TAPSE to predict the R-CHF onset in dogs with MMVD

Variable	AUC	Cutoff	Sensitivity (%)	Specificity (%)
RVIDd	0.88 (0.75-0.99)	12.9	.80	.82
RVEDA	0.76 (0.60-0.93)	2.9	.73	.73
RVESA	0.76 (0.58-0.94)	1.6	.79	.73
RVWTd	0.88 (0.79-0.97)	4.0	.76	.91
$TAPSE_{B\text{-}mode}$	0.52 (0.31-0.66)	11.2	.55	.55
$TAPSE_{B\text{-}mode}$/Ao	0.51 (0.30-0.69)	0.80	.55	.55
$TAPSE_{B\text{-}mode}$/RVIDd	0.90 (0.81-0.97)	0.78	.84	.82
$TAPSE_{B\text{-}mode}$/RVEDA	0.81 (0.67-0.95)	4.0	.75	.91
$TAPSE_{B\text{-}mode}$/RVESA	0.75 (0.58-0.92)	5.6	.89	.64
$TAPSE_{B\text{-}mode}$/RVWTd	0.81 (0.70-0.91)	2.8	.66	.91
$TAPSE_{M\text{-}mode}$	0.59 (0.42-0.76)	9.5	.49	.82
$TAPSE_{M\text{-}mode}$/Ao	0.63 (0.45-0.82)	0.86	.71	.64
$TAPSE_{M\text{-}mode}$/RVIDd	0.83 (0.70-0.96)	0.69	.84	.82
$TAPSE_{M\text{-}mode}$/RVEDA	0.74 (0.57-0.90)	3.8	.74	.82
$TAPSE_{M\text{-}mode}$/RVESA	0.74 (0.55-0.92)	5.4	.88	.64
$TAPSE_{M\text{-}mode}$/RVWTd	0.71 (0.54-0.88)	2.4	.68	.73

Abbreviations: AUC, area under the curve; MMVD, myxomatous mitral valve disease; R-CHF, right-sided congestive heart failure; RV, right ventricular; RVEDA, right ventricular end-diastolic area; RVESA, right ventricular end-systolic area; RVIDd, end-diastolic right ventricular diameter; RV-SL; right ventricular peak strain; RVWTd, right ventricular end-diastolic wall thickness; TAPSE, tricuspid annular plane systolic excursion; TR, tricuspid regurgitation; VHS, vertebral heart size.

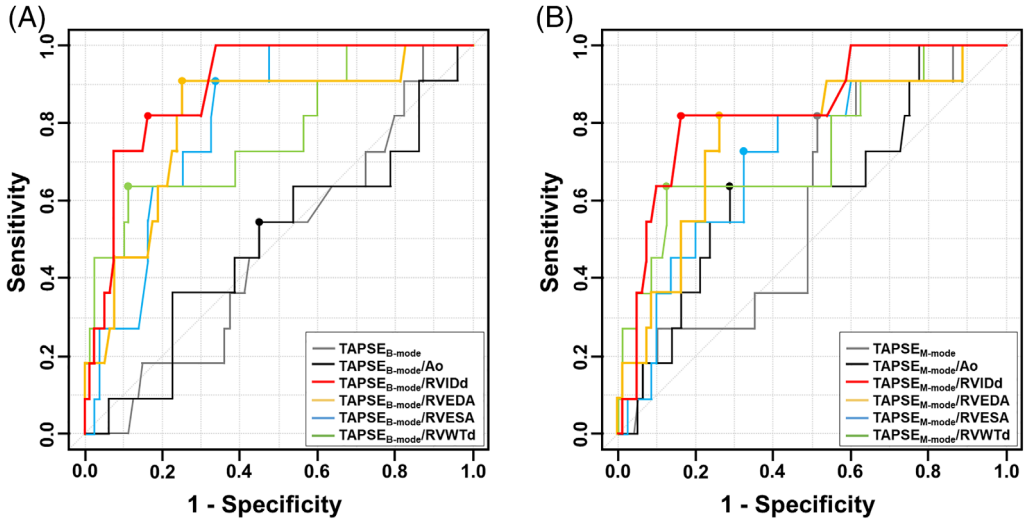

FIGURE 3 Receiver operating characteristic curves of the nonnormalized TAPSE and TAPSE normalized by each RV size indicators to predict R-CHF onset: $TAPSE_{B\text{-}mode}$, A, and $TAPSE_{M\text{-}mode}$, B. Gray line represents TAPSE, black line represents TAPSE/Ao, red line represents TAPSE/RVIDd, orange line represents TAPSE/RVEDA, blue line represents TAPSE/RVESA, and green line represents TAPSE/RVWTd. The optimal cutoff value was defined as that which minimized the distance between the curve and upper left corner in the receiver operating characteristic curve. R-CHF, right-sided congestive heart failure; RV, right ventricular; RVEDA, right ventricular end-diastolic area; RVESA, right ventricular end-systolic area; RVIDd, end-diastolic right ventricular diameter; RVWTd, right ventricular end-diastolic wall thickness; TAPSE, tricuspid annular plane systolic excursion; TAPSE/Ao, tricuspid annular plane systolic excursion-to-aortic diameter ratio

especially $TAPSE_{B\text{-}mode}$/RVIDd, RVIDd, and RVWTd showed significantly high AUC, sensitivity, and specificity. In addition, linear regression analysis showed moderate positive correlations between $TAPSE_{B\text{-}mode}$/RVIDd and $RV\text{-}SL_{3seg}$, and between $TAPSE_{B\text{-}mode}$/RVIDd and $RV\text{-}SL_{6seg}$ (Figure 4).

3.3 | Intraobserver and interobserver measurement variability

Table 6 shows the results of interobserver and intraobserver measurement of variability obtained from RV morphological and

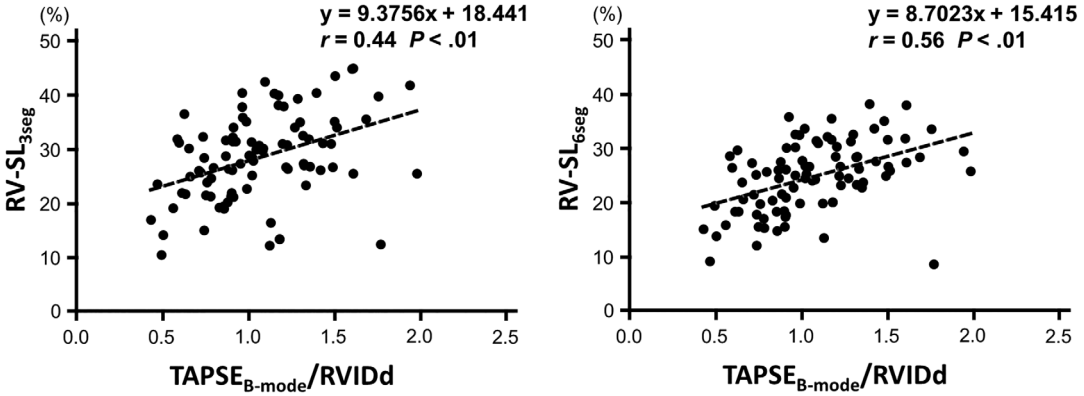

FIGURE 4 Correlations between $TAPSE_{B\text{-}mode}$/RVIDd and $RV\text{-}SL_{3seg}$, A, and $RV\text{-}SL_{6seg}$, B. 3seg, only right ventricular free wall; 6seg, right ventricular free wall and interventricular septum; RVIDd, end-diastolic right ventricular diameter; RV-SL; right ventricular peak strain; TAPSE, tricuspid annular plane systolic excursion

TABLE 6 Intraobserver and interobserver measurement variability for RV morphological and functional indicators

	Intraobserver			Interobserver		
Variables	**CV (%)**	**ICC (1,1)**	***P***	**CV (%)**	**ICC (2,1)**	***P***
RVIDd	3.6	0.96	<.01	7.4	0.91	<.01
RVEDA	4.1	0.99	<.01	9.0	0.76	<.01
RVESA	5.8	0.94	<.01	22.3	0.50	.01
RVWTd	4.1	0.89	<.01	5.6	0.76	<.01
$TAPSE_{B\text{-}mode}$	3.3	0.90	<.01	5.9	0.80	<.01
$TAPSE_{B\text{-}mode}$/Ao	3.6	0.88	<.01	5.6	0.88	<.01
$TAPSE_{B\text{-}mode}$/RVIDd	5.3	0.90	<.01	6.7	0.95	<.01
$TAPSE_{B\text{-}mode}$/RVEDA	6.2	0.92	<.01	9.8	0.90	<.01
$TAPSE_{B\text{-}mode}$/RVESA	8.5	0.95	<.01	20.8	0.95	<.01
$TAPSE_{B\text{-}mode}$/RVWTd	5.3	0.95	.05	10.6	0.56	.05
$TAPSE_{M\text{-}mode}$	6.5	0.68	<.01	8.5	0.59	.13
$TAPSE_{M\text{-}mode}$/Ao	7.1	0.71	<.01	8.8	0.77	.01
$TAPSE_{M\text{-}mode}$/RVIDd	8.1	0.75	<.01	11.4	0.73	.04
$TAPSE_{M\text{-}mode}$/RVEDA	7.3	0.72	<.01	12.5	0.92	<.01
$TAPSE_{M\text{-}mode}$/RVESA	9.9	0.96	<.01	24.8	0.92	<.01
$TAPSE_{M\text{-}mode}$/RVWTd	7.5	0.94	<.01	11.1	0.42	.11
$RV\text{-}SL_{3seg}$	4.4	0.93	<.01	4.9	0.91	<.01
$RV\text{-}SL_{6seg}$	5.2	0.90	<.01	6.9	0.84	<.01

Abbreviations: 3seg, only right ventricular free wall; 6seg, right ventricular free wall and interventricular septum; AUC, area under the curve; CV, coefficient of variation; ICC, intraclass correlation coefficients; MMVD, myxomatous mitral valve disease; RV, right ventricular; RVEDA, right ventricular end-diastolic area; RVESA, right ventricular end-systolic area; RVIDd, end-diastolic right ventricular diameter; RV-SL; right ventricular peak strain; RVWTd, right ventricular end-diastolic wall thickness; TAPSE, tricuspid annular plane systolic excursion; TR, tricuspid regurgitation; VHS, vertebral heart size.

functional indices. For the RV morphological indices, RVIDd and RVWTd showed good reproducibility according to CV >10.0 and ICC >0.7. In terms of TAPSE, TAPSE measured using B-mode had better reproducibility compared with that measured using M-mode. The TAPSE normalized using the RV size showed good reproducibility in all cases for intraobserver and interobserver measurement of variability, and $TAPSE_{B\text{-}mode}$/RVIDd, especially, showed good reproducibility.

4 | DISCUSSION

In our study, although nonnormalized TAPSE and TAPSE/Ao measured using the B-mode and M-mode methods were higher in the mild and moderate PH groups compared with the normal group, no significant changes were observed in the severe PH group. A previous report that included a majority of dogs with precapillary PH and some

dogs with postcapillary PH found that TAPSE was higher in the mild to moderate groups and lower in the severe PH group.[15] The study concluded that decreased TAPSE may be caused by severe pressure overload in the severe PH groups and might reflect RV systolic dysfunction.[15] However, other studies indicated that TAPSE could be increased by volume overload through various mechanisms, such as Starling's law of the heart.[9,15,19-21] Our results also suggest that the increase in volume overload and the decrease in pressure overload associated with TR might increase TAPSE in dogs with postcapillary PH. Furthermore, ventricular interdependence also might affect TAPSE, especially in dogs with severe MMVD.[19] Therefore, our results suggest that nonnormalized TAPSE measured using B-mode and M-mode methods could not detect RV systolic dysfunction because of severe volume overload associated with TR and ventricular interdependence in dogs with MMVD.

On the other hand, TAPSE normalized using each RV size index, increasing in the mild PH group and decreasing in the severe PH group. Severe pressure overload and consequent RV systolic dysfunction in the severe PH group also may cause the decrease in normalized TAPSE.[15] In our study, almost all dogs with severe PH had not only pressure overload but also volume overload because of TR. Because RV dilatation was closely associated with TR jet area (RV volume overload), TAPSE increases along with the increased volume overload.[20,42] However, the TAPSE divided by RV size indices did not increase in the severe PH group, although it did increase in the mild PH group. Our results indicate that TAPSE normalized using RV size indices might detect the RV contractile performance regardless of the change in load condition, and hence could be a useful tool to assess RV systolic function, that could not be detected by nonnormalized TAPSE in dogs with postcapillary PH.

The RV-SL obtained in our study, especially RV-SL_{6seg}, also was higher in the mild PH group compared with that of the normal group and was lower in the severe PH group compared with that of the mild PH group. We previously have reported that left ventricular myocardial function (including the interventricular septum) might be worsened in dogs with MMVD.[25,43] Because the left and right ventricle share the interventricular septum, decreased left ventricular function associated with MMVD might affect function in the interventricular septum as in the right ventricle. In addition, another study indicated that the interventricular septum plays an important role in RV ejection.[44] Therefore, our results suggest that RV-SL_{6seg} could reflect dysfunction of the entire RV myocardium more sensitively. Moreover, linear regression analysis indicated that the $TAPSE_{B\text{-}mode}$/RVIDd ratio had moderate positive correlation with RV-SL. Because the 2D-STE method precisely reflects myocardial expansion and contraction,[45] TAPSE normalized using RV size might detect the force of myocardial contraction. Therefore, it can be presumed that normalized TAPSE might reflect RV myocardial compensation and decompensation in detail against RV load, as observed in the RV-SL.

In our study, $TAPSE_{B\text{-}mode}$ showed more significant decrease and better reproducibility than did $TAPSE_{M\text{-}mode}$. We considered that the motion of the tricuspid annulus in 3 dimensions should be measured for evaluating RV systolic function because it is considered difficult to evaluate RV function only in the longitudinal direction obtained from RV focus view owing to its complex structure.[46,47] In human medicine, RV circumferential function also would contribute to RV systolic function in addition to longitudinal function.[48] Furthermore, a recent study reported the importance of radial RV function in dogs with PH.[49] Therefore, we measured $TAPSE_{B\text{-}mode}$ as 2D total displacement (not parallel to the RV longitudinal direction at end-diastole) with reference to the previous study that assessed $TAPSE_{B\text{-}mode}$ in humans, although the previous report that used dogs with MMVD assessed $TAPSE_{B\text{-}mode}$ parallel to the RV longitudinal direction.[13,22] Therefore, our results suggest that $TAPSE_{B\text{-}mode}$ might be more sensitive to RV systolic dysfunction than is $TAPSE_{M\text{-}mode}$. In addition, these indices could not be used interchangeably, especially in dogs with severe postcapillary PH.

For results comparing TAPSE in the presence or absence of R-CHF, only normalized TAPSE measured by both methods showed a significant decrease in dogs with R-CHF, although nonnormalized TAPSE showed no significant decrease. The TAPSE normalized using RVIDd had the highest AUC, sensitivity, and specificity to predict R-CHF onset compared with the other normalized indices. In addition, multivariate analysis indicated that $TAPSE_{B\text{-}mode}$/RVIDd and LA/Ao ratios were significant independent predictors. In human medicine, RV linear dimension provided readily obtainable markers of RV chamber size and was independently associated with RV volumes on cardiac magnetic resonance imaging.[50] Furthermore, RVIDd used in our study does not need to take into account the low echocardiographic image resolution in the near-field from the probe.[51] Therefore, although RV morphological indices also had high AUC to predict R-CHF onset, the $TAPSE_{B\text{-}mode}$/RVIDd ratio may be an additional tool to estimate the R-CHF onset with high sensitivity and specificity.

Our study had several limitations. First, the effects of medication could not be considered in dogs with MMVD. Some drugs such as pimobendan, pulmonary vasodilators, and diuretics might affect RV function indices by changing the pressure and volume loads against the right heart. Second, the dogs were diagnosed with PH based on the TR velocity, although catheterization is the gold standard for PH diagnosis. In addition, excessively impaired RV function may lead to the underestimation of peak TR velocity and PH severity. Finally, our sample size was relatively small, especially dogs with moderate-to-severe PH and the R-CHF groups. Unfortunately, there were only a few dogs with postcapillary PH that might progress to pulmonary vascular remodeling secondary to MMVD. Our study however could assess and compare the precise RV function of dogs with PH secondary to MMVD.

In conclusion, TAPSE normalized by RV size might reflect RV systolic dysfunction in dogs with severe PH, which could not be detected by the nonnormalized TAPSE because of its load dependency and ventricular interdependence. In addition, $TAPSE_{B\text{-}mode}$/RVIDd ratio could be a useful tool for predicting R-CHF onset with high sensitivity and specificity. Additional studies that involve more dogs with severe PH should be performed to evaluate the utility of normalized TAPSE.

ACKNOWLEDGMENT

No funding was received for this study. This research was presented as an ePoster at the 2020 ACVIM Forum On Demand. The authors express their deepest appreciation to Haruka Kanno for her technical assistance. In addition, we thank Editage (www.editage.com) for English language editing.

CONFLICT OF INTEREST DECLARATION

Authors declare no conflict of interest.

OFF-LABEL ANTIMICROBIAL DECLARATION

Authors declare no off-label use of antimicrobials.

INSTITUTIONAL ANIMAL CARE AND USE COMMITTEE (IACUC) OR OTHER APPROVAL DECLARATION

Authors declare no IACUC or other approval was needed.

HUMAN ETHICS APPROVAL DECLARATION

Authors declare human ethics approval was not needed for this study.

ORCID

Yunosuke Yuchi https://orcid.org/0000-0002-6293-7320
Ryohei Suzuki https://orcid.org/0000-0001-9451-5854

REFERENCES

1. Gaynor SL, Maniar HS, Bloch JB, et al. Right atrial and ventricular adaptation to chronic right ventricular pressure overload. *Circulation*. 2005;112:212-218.
2. Vonk-Noordegraaf A, Haddad F, Chin KM, et al. Right heart adaptation to pulmonary arterial hypertension: physiology and pathobiology. *J Am Coll Cardiol*. 2013;62:22-33.
3. Kellihan HB, Stepien RL. Pulmonary hypertension in canine degenerative mitral valve disease. *J Vet Cardiol*. 2012;14:149-164.
4. Reinero C, Visser LC, Kellihan HB, et al. ACVIM consensus statement guidelines for the diagnosis, classification, treatment, and monitoring of pulmonary hypertension in dogs. *J Vet Intern Med*. 2020;34:549-573.
5. Borgarelli M, Abbott J, Braz-Ruivo L, et al. Prevalence and prognostic importance of pulmonary hypertension in dogs with myxomatous mitral valve disease. *J Vet Intern Med*. 2015;29:569-574.
6. Assad TR, Hemnes AR, Larkin EK, et al. Clinical and biological insights into combined post- and pre-capillary pulmonary hypertension. *J Am Coll Cardiol*. 2016;68:2525-2536.
7. Hoeper MM, Bogaard HJ, Condliffe R, et al. Definitions and diagnosis of pulmonary hypertension. *J Am Coll Cardiol*. 2013;62:D42-D50.
8. Tidholm A, Höglund K, Häggström J, Ljungvall I. Diagnostic value of selected echocardiographic variables to identify pulmonary hypertension in dogs with myxomatous mitral valve disease. *J Vet Intern Med*. 2015;29:1510-1517.
9. Chapel EH, Scansen BA, Schober KE, Bonagura JD. Echocardiographic estimates of right ventricular systolic function in dogs with myxomatous mitral valve disease. *J Vet Intern Med*. 2018;32:64-71.
10. Soydan LC, Kellihan HB, Bates ML, et al. Accuracy of Doppler echocardiographic estimates of pulmonary artery pressures in a canine model of pulmonary hypertension. *J Vet Cardiol*. 2015;17:13-24.
11. Caivano D, Rishniw M, Birettoni F, et al. Right ventricular outflow tract fractional shortening: an echocardiographic index of right ventricular systolic function in dogs with pulmonary hypertension. *J Vet Cardiol*. 2018;20:354-363.
12. Visser LC, Scansen BA, Schober KE, Bonagura JD. Echocardiographic assessment of right ventricular systolic function in conscious healthy dogs: repeatability and reference intervals. *J Vet Cardiol*. 2015;17:83-96.
13. Visser LC, Sintov DJ, Oldach MS. Evaluation of tricuspid annular plane systolic excursion measured by two-dimensional echocardiography in healthy dogs: repeatability, reference intervals, and comparison with M-mode assessment. *J Vet Cardiol*. 2018;20:165-174.
14. Chetboul V, Damoiseaux C, Lefebvre HP, et al. Quantitative assessment of systolic and diastolic right ventricular function by echocardiography and speckle-tracking imaging: a prospective study in 104 dogs. *J Vet Sci*. 2018;19:683-692.
15. Pariaut R, Saelinger C, Strickland KN, Beaufrère H, Reynolds CA, Vila J. Tricuspid annular plane systolic excursion (TAPSE) in dogs: reference values and impact of pulmonary hypertension. *J Vet Intern Med*. 2012;26:1148-1154.
16. Sato T, Tsujino I, Oyama-Manabe N, et al. Simple prediction of right ventricular ejection fraction using tricuspid annular plane systolic excursion in pulmonary hypertension. *Int J Cardiovasc Imaging*. 2013;29:1799-1805.
17. López-Candales A, Rajagopalan N, Saxena N, Gulyasy B, Edelman K, Bazaz R. Right ventricular systolic function is not the sole determinant of tricuspid annular motion. *Am J Cardiol*. 2006;98:973-977.
18. Ghio S, Temporelli PL, Klersy C, et al. Prognostic relevance of a non-invasive evaluation of right ventricular function and pulmonary artery pressure in patients with chronic heart failure. *Eur J Heart Fail*. 2013;15:408-414.
19. Poser H, Berlanda M, Monacolli M, Contiero B, Coltro A, Guglielmini C. Tricuspid annular plane systolic excursion in dogs with myxomatous mitral valve disease with and without pulmonary hypertension. *J Vet Cardiol*. 2017;19:228-239.
20. Morita T, Nakamura K, Osuga T, et al. Effect of acute volume overload on echocardiographic indices of right ventricular function and dyssynchrony assessed by use of speckle tracking echocardiography in healthy dogs. *Am J Vet Res*. 2019;80:51-60.
21. Hsiao S-H, Lin S-K, Wang W-C, Yang SH, Gin PL, Liu CP. Severe tricuspid regurgitation shows significant impact in the relationship among peak systolic tricuspid annular velocity, tricuspid annular plane systolic excursion, and right ventricular ejection fraction. *J Am Soc Echocardiogr*. 2006;19:902-910.
22. Naoum EE, Schofield PT, Shen T, Andrawes MN, Kuo AS. Agreement between transesophageal echocardiographic tricuspid annular plane systolic excursion measurement methods in cardiac surgery patients. *J Cardiothorac Vasc Anesth*. 2019;33:717-724.
23. Caivano D, Dickson D, Pariaut R, Stillman M, Rishniw M. Tricuspid annular plane systolic excursion-to-aortic ratio provides a bodyweight-independent measure of right ventricular systolic function in dogs. *J Vet Cardiol*. 2018;20:79-91.
24. Dandel M, Hetzer R. Echocardiographic assessment of the right ventricle: impact of the distinctly load dependency of its size, geometry and performance. *Int J Cardiol*. 2016;221:1132-1142.
25. Suzuki R, Matsumoto H, Teshima T, Koyama H. Clinical assessment of systolic myocardial deformations in dogs with chronic mitral valve insufficiency using two-dimensional speckle-tracking echocardiography. *J Vet Cardiol*. 2013;15:41-49.
26. Acierno MJ, Brown S, Coleman AE, et al. ACVIM consensus statement: guidelines for the identification, evaluation, and management of systemic hypertension in dogs and cats. *J Vet Intern Med*. 2018;32:1803-1822.
27. Keene BW, Atkins CE, Bonagura JD, et al. ACVIM consensus guidelines for the diagnosis and treatment of myxomatous mitral valve disease in dogs. *J Vet Intern Med*. 2019;33:1127-1140.

28. Vezzosi T, Domenech O, Costa G, et al. Echocardiographic evaluation of the right ventricular dimension and systolic function in dogs with pulmonary hypertension. *J Vet Intern Med*. 2018;32:1541-1548.
29. Lancellotti P, Moura L, Pierard LA, et al. European association of echocardiography recommendations for the assessment of valvular regurgitation. Part 2: mitral and tricuspid regurgitation (native valve disease). *Eur J Echocardiogr*. 2010;11:307-332.
30. Buchanan JW, Bücheler J. Vertebral scale system to measure canine heart size in radiographs. *JAMA*. 1995;206:194-199.
31. Lisciandro GR. The use of the diaphragmatico-hepatic (DH) views of the abdominal and thoracic focused assessment with sonography for triage (AFAST/TFAST) examinations for the detection of pericardial effusion in 24 dogs (2011-2012). *J Vet Emerg Crit Care*. 2016;26:125-131.
32. Vientós-Plotts AI, Wiggen KE, Lisciandro GR, Reinero CR. The utility of point-of-care ultrasound right-sided cardiac markers as a screening test for moderate to severe pulmonary hypertension in dogs. *Vet J*. 2019;250:6-13.
33. Hansson K, Häggström J, Kvart C, et al. Left atrial to aortic root indices using two-dimensional and M-mode echocardiography in cavalier King Charles Spaniels with and without left atrial enlargement. *Vet Radiol Ultrasound*. 2002;43:568-575.
34. Visser LC, Ciccozzi MM, Sintov DJ, Sharpe AN. Echocardiographic quantitation of left heart size and function in 122 healthy dogs: a prospective study proposing reference intervals and assessing repeatability. *J Vet Intern Med*. 2019;33:1909-1920.
35. Rishniw M, Caivano D, Dickson D, Vatne L, Harris J, Matos JN. Two-dimensional echocardiographic left- atrial-to-aortic ratio in healthy adult dogs: a reexamination of reference intervals. *J Vet Cardiol*. 2019;26:29-38.
36. Cornell CC, Kittleson MD, Della Torre P, et al. Allometric scaling of M-mode cardiac measurements in normal adult dogs. *J Vet Intern Med*. 2004;18:311-321.
37. Rudski LG, Lai WW, Afilalo J, et al. Guidelines for the echocardiographic assessment of the right heart in adults: a report from the American Society of Echocardiography. Endorsed by the European Association of Echocardiography, a registered branch of the European Society of Cardiology, and. *J Am Soc Echocardiogr*. 2010;23:685-713.
38. Gentile-Solomon JM, Abbott JA. Conventional echocardiographic assessment of the canine right heart: reference intervals and repeatability. *J Vet Cardiol*. 2016;18:234-247.
39. Currie PJ, Seward JB, Chan KL, et al. Continuous wave Doppler determination of right ventricular pressure: a simultaneous Doppler-catheterization study in 127 patients. *J Am Coll Cardiol*. 1985;6:750-756.
40. Kanda Y. Investigation of the freely available easy-to-use software "EZR" for medical statistics. *Bone Marrow Transplant*. 2013;48:452-458.
41. Fischer JE, Bachmann LM, Jaeschke R. A readers' guide to the interpretation of diagnostic test properties: clinical example of sepsis. *Intensive Care Med*. 2003;29:1043-1051.
42. Hinderliter AL, Willis PW, Long WA, et al. Frequency and severity of tricuspid regurgitation determined by Doppler echocardiography in primary pulmonary hypertension. *Am J Cardiol*. 2003;91:1033-1037.
43. Suzuki R, Matsumoto H, Teshima T, Koyama H. Noninvasive clinical assessment of systolic torsional motions by two-dimensional speckle-tracking echocardiography in dogs with myxomatous mitral valve disease. *J Vet Intern Med*. 2013;27:69-75.
44. Starr I, Jeffers WA, Meade RH. The absence of conspicuous increments of venous pressure after severe damage to the right ventricle of the dog, with a discussion of the relation between clinical congestive failure and heart disease. *Am Heart J*. 1943;26:291-301.
45. Culwell NM, Bonagura JD, Schober KE. Comparison of echocardiographic indices of myocardial strain with invasive measurements of left ventricular systolic function in anesthetized healthy dogs. *Am J Vet Res*. 2011;72:650-660.
46. Jenkins C, Chan J, Bricknell K, Strudwick M, Marwick TH. Reproducibility of right ventricular volumes and ejection fraction using real-time three-dimensional echocardiography: comparison with cardiac MRI. *Chest*. 2007;131:1844-1851.
47. Sieslack AK, Dziallas P, Nolte I, Wefstaedt P, Hungerbühler SO. Quantification of right ventricular volume in dogs: a comparative study between three-dimensional echocardiography and computed tomography with the reference method magnetic resonance imaging. *BMC Vet Res*. 2014;10:242.
48. Vitarelli A, Terzano C. Do we have two hearts? New insights in right ventricular function supported by myocardial imaging echocardiography. *Heart Fail Rev*. 2010;15:39-61.
49. Caivano D, Rishniw M, Birettoni F, et al. Transverse right ventricle strain and strain rate assessed by 2-dimensional speckle tracking echocardiography in dogs with pulmonary hypertension. *Vet Sci*. 2020;7:1-10.
50. Kim J, Srinivasan A, Seoane T, et al. Echocardiographic linear dimensions for assessment of right ventricular chamber volume as demonstrated by cardiac magnetic resonance. *J Am Soc Echocardiogr*. 2016;29:861-870.
51. Bleeker GB, Steendijk P, Holman ER, et al. Assessing right ventricular function: the role of echocardiography and complementary technologies. *Heart*. 2006;92:19-26.

How to cite this article: Yuchi Y, Suzuki R, Teshima T, Matsumoto H, Koyama H. Utility of tricuspid annular plane systolic excursion normalized by right ventricular size indices in dogs with postcapillary pulmonary hypertension. *J Vet Intern Med*. 2021;35:107–119. https://doi.org/10.1111/jvim.15984